



Scientific Workshop on Nuclear Fission dynamics and the Emission of Prompt Neutrons and Gamma Rays, THEORY-3

A sample of the results of the first SOFIA experiment

T. Gorbinet^{a,b}, G. Bélier^a, G. Boutoux^a, A. Chatillon^a, A. Ebran^a, B. Laurent^a, J.-F. Martin^a, E. Pellereau^a, J. Taieb^a, L. Audouin^b, L. Tassan-Got^b, B. Jurado^c, H. Álvarez-Pol^d, Y. Ayyad^d, J. Benlliure^d, M. Caamaño^d, D. Cortina-Gil^d, B. Fernández-Domínguez^d, C. Paradela^d, J.-L. Rodríguez-Sánchez^d, J. Vargas^d, E. Casarejos^e, A. Heinz^f, A. Kelić-Heil^g, N. Kurz^g, C. Nociforo^g, S. Pietri^g, A. Prochazka^g, D. Rossi^g, K.-H. Schmidt^g, H. Simon^g, B. Voss^g, H. Weick^g, J.S. Winfield^g

^aCEA, DAM, DIF, Arpajon, France

^bCNRS, IPN Orsay, Orsay, France

^cCNRS, CENBG, Gradignan, France

^dUniversidade de Santiago de Compostela, Spain

^eUniversidade de Vigo, Spain

^fChalmers University of Technology, Gothenburg, Sweden

^gGSI, Darmstadt, Germany

Abstract

The first SOFIA experiment (Studies On Fission with Aladin) was performed in August 2012 at GSI. The fission of several neutron-deficient actinides and pre-actinides was induced in flight at 700 A MeV by electromagnetic excitation. The use of inverse kinematics provides both high detection and high geometrical efficiency. The complete identification of both fission fragments in coincidence (nuclear charge and mass) was obtained over a broad range of fissioning nuclei. After a short introduction and description of the experimental setup, the quality of the charge and mass separation is presented, followed by some results concerning the Coulex-induced fission of ²³⁴U and ²³⁵U.

© 2015 Published by Elsevier B.V. This is an open access article under the CC BY-NC-ND license

(<http://creativecommons.org/licenses/by-nc-nd/4.0/>).

Peer-review under responsibility of the European Commission, Joint Research Centre – Institute for Reference Materials and Measurements

Keywords: Electromagnetic-induced fission ; Isotopic yields ; Inverse kinematics ; Relativistic secondary radioactive beams

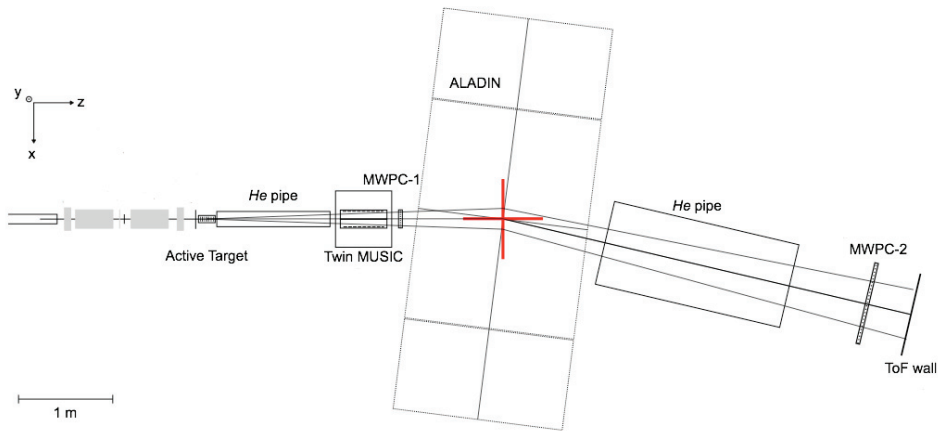


Fig. 1. SOFIA setup in Cave C: Fission of the incoming nuclei occurs in the Active Target (AT). Detectors upstream the AT are dedicated to the identification of the fissioning system and detectors downstream, surrounding the ALADIN dipole, to the identification in (Z,A) of the fission fragments.

1. Overview of SOFIA

Nuclear applications require more and more precise simulations, which subsequently means more and more precise nuclear data. Fission fragments yields are a necessary input for simulation codes, especially for the predictions on safety and waste management issues. SOFIA is one of a very few innovative experimental programs aiming at studying fission fragment isotopic distributions. Fission yields can be inferred in neutron-induced experiments using actinide targets. However, direct-kinematics measurements suffer from two main drawbacks. First is the limitation of such studies to long-lived actinides because of restrictions on availability, handling and purity of targets. Second is the impossibility to get the charge of the heavy fragment with sufficient resolution due to charge-state fluctuations inside the detectors. The use of inverse kinematics technique at relativistic energies overcome these difficulties. Indeed, short-lived actinides (down to $1\mu s$) radioactive beams can be produced and Lorentz boost applied to fission fragments ease the charge identification by getting rid of charge-state fluctuations inside the detectors. GSI is the unique worldwide facility capable of providing a ^{238}U primary beam at an energy of 1 GeV per nucleon needed to produce secondary radioactive beams at high energy. The secondary cocktail beam is produced by fragmentation of the primary beam on a beryllium target. Nuclei of interest are separated in-flight by the high-resolution magnetic spectrometer FRS and are transmitted to Cave C, where fission occurs. By choosing a specific magnetic rigidity for the FRS, the transmission is limited to several isotopes with a similar A/q ratio (mass over ionic charge), following the equation of motion of a charged particle in a uniform magnetic field B :

$$B\rho = \frac{p}{q} \propto \frac{A}{q} \beta\gamma \quad (1)$$

where ρ is the deflection radius, p the momentum, β the relative velocity and γ the Lorentz factor. The first part of the setup is dedicated to the identification of this secondary beam via the $B\rho - \Delta E - \text{ToF}$ method. $B\rho$ is deduced from

* Corresponding author.

E-mail address: gorbinet@ipno.in2p3.fr / thomas.gorbinet@gmail.com

the tracking of the ions. The nuclear charge Z is determined by measuring the energy loss ΔE in Multi-Sampling Ionization Chambers (MUSIC). The reduced momentum $\beta\gamma$ is given by a time-of-flight *ToF* measurement between the FRS and Cave C. The mass is then computed using equation (1). Fission takes place in the Active Target, a stack of small ionization chambers in which the cathodes are the targets: two thick uranium targets to maximize reaction rate and one thin lead target for precise Total Kinetic Energy (TKE) measurement. The excitation energy is not known accurately but the electromagnetic excitation function is mainly governed by the Giant Dipole Resonance (GDR) with a mean value around 12 *MeV*. The second part of the setup, shown in Fig.1, is dedicated to the identification of the fission fragments themselves using the same $B\rho - \Delta E - ToF$ technique. The nuclear charge of each fission fragment is deduced from 10 successive energy loss measurements in a Twin MUSIC filled with a custom gas to increase drift velocity and reduce longitudinal diffusion. The Twin MUSIC also provides a highly accurate entrance angle of the fragments in the dipole thanks to the 10 consecutive drift time measurements. The resolution achieved is less than 2 *mrad* full width at half maximum (FWHM). The trajectory of the fission fragments used to determine their magnetic rigidity is obtained by a combination of this angle and two position measurements using Multi-Wire Proportional Chambers (MWPC) in front of and behind the ALADIN dipole. The time-of-flight is measured on a 7.5 *m* flight path between a small plastic scintillator in front of the target and a time-of-flight wall (ToF-wall) made of 28 plastic scintillators at the end of the setup. The time resolution is crucial in this experiment since 40 *ps* FWHM are required to get resolved masses. New VFTX Time-to-Digital Converters (TDC) with 17 *ps* FWHM intrinsic resolution have been developed by GSI and CEA Bruyères-le-Châtel for this purpose and a detailed study on the technological choice for plastics and photomultiplier tubes (PMT) has been made and published in [Ebran et al. (2013)]. A more exhaustive description of the setup can be found in [Pellereau et al. (2013)] and [Boutoux et al. (2013)].

2. Charge and mass separation of the fission fragments

2.1. Charge distribution

The nuclear charge Z of each fission fragment is obtained from corrected ΔE measurements in the Twin MUSIC. Indeed at fixed Z , ΔE depends on the velocity of the fragment and on its transverse position due to electron recombination along the drift path inside the detector. The charge distribution obtained for the fission of ^{235}U (both electromagnetic and nuclear) is given in Fig.2 (a). Plotting this distribution unveils well-separated peaks with a resolution of 0.4 unit FWHM and unambiguous signature of even-odd staggering of the fragments. The data acquisition is triggered when two fragments hit the ToF-wall, thus not only Coulex-induced fissions are recorded. In order to clean the data, the nuclear contribution, which comes mostly from high-energy fissions, has to be removed. High-energy fissions being usually preceded by the emission of light charged particles, the first requirement is to select events such that the sum of the charges of the fragments is equal to the charge of the fissioning nuclei. However, the resulting data are still polluted by a fraction of nuclear-induced fissions for which only neutrons are emitted before fission. To get rid of this contamination, the nuclear-charge distribution obtained from nuclear-induced fission in the aluminium anodes of the Active Target is weighted appropriately and subtracted, under the hypothesis of limited fragmentation regime and factorization [Heckman et al. (1972)].

2.2. Mass distribution

As previously explained, the mass A of each fission fragment is deduced from a combination of their charge, velocity and magnetic rigidity. The time measurement used to compute the velocity is sensitive to the amplitude of the signal despite the use of Constant Fraction Discriminators (walk effect). For a given fragment, the amplitude of the signal on the PMT varies with the position of the hit in the plastic scintillator, due to light attenuation in the material. The resulting variation in the measured time can reach 200 *ps*, enough to shift the measured mass number by 2.5 units. An accurate correction is performed to obtain the true mass distribution shown in Fig.2 (b) for ^{235}U . The resolution is around 0.6 unit FWHM for the light fragment group ($A \approx 95$) and 0.8 unit FWHM for the heavy fragment group ($A \approx 135$).

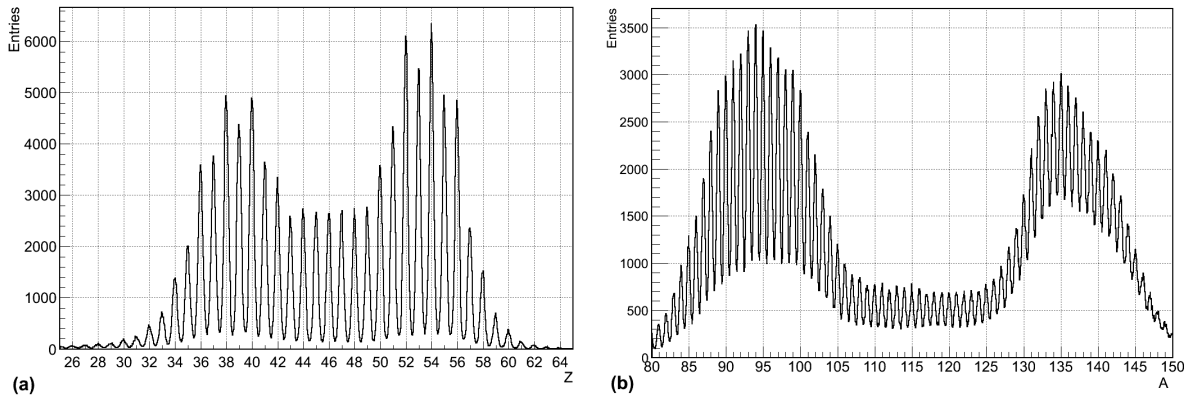


Fig. 2. Selection on ^{235}U beam, fission events in the Active Target - (a) Charge distribution ; (b) Mass distribution

3. Comparison of ^{234}U fission yields with existing experimental data, evaluations and codes

3.1. Comparison to data

The isobaric yields for the Coulex-induced fission of ^{234}U are represented in Fig.3 (a) and compared to thermal neutron-induced fission of ^{233}U measured at ILL, Grenoble, [Quade et al. (1988)] and [Martin et al. (2014)]. Thermal neutron-induced fission exhibits a more asymmetric behavior, the symmetric valley being completely depleted. This symmetric component plays on the opposite a non negligible role in Coulex-induced fission for which the excitation energy is higher. On the lighter fragments group, one observes the same fine structure for both sets of data with an enhancement of the yields around $A = 90$ and $A = 94$. It seems that such fine structure effects do not depend on the excitation energy.

3.2. Comparison to evaluations

The mean excitation energy in Coulex-induced fission has been estimated to 12 MeV , which corresponds to the absorption of a $\approx 6\text{ MeV}$ neutron. The European JEFF 3.1.1. library contains, among others, evaluation for $^{233}\text{U}(n, f)$ at 400 keV (epithermal neutrons) and 14 MeV (fast neutrons). Fig.3 (b) shows the comparison between these two sets of evaluated data and SOFIA data. As expected, the SOFIA data stands between both evaluations. The increase of the contribution of the symmetric component while increasing the neutron(-equivalent) energy is clearly visible. The feature previously discussed regarding the fine structure on the lighter fragments group, and the excitation energy-independent enhancement of specific mass values is also observed.

3.3. Comparison to codes

The SOFIA elemental fission yields have been compared in Fig.3 (c) to a calculation performed by the semi-empirical code GEF [Schmidt et al. (2014)] for the fission of the compound nucleus ^{234}U . The overall agreement is excellent with slight discrepancies regarding the proportion of symmetric fission and the importance of the even-odd staggering.

4. Preliminary results on total prompt neutron multiplicity and total kinetic energy for $^{235}\text{U}(\text{coulex}, f)$

4.1. Total prompt neutron multiplicity

The total prompt neutron multiplicity ν is deduced in SOFIA data on an event-by-event basis by simply subtracting the sum of the masses of the fragments $A_{FF1} + A_{FF2}$ to the mass of the fissioning nuclei A : $\nu = A - (A_{FF1} + A_{FF2})$.

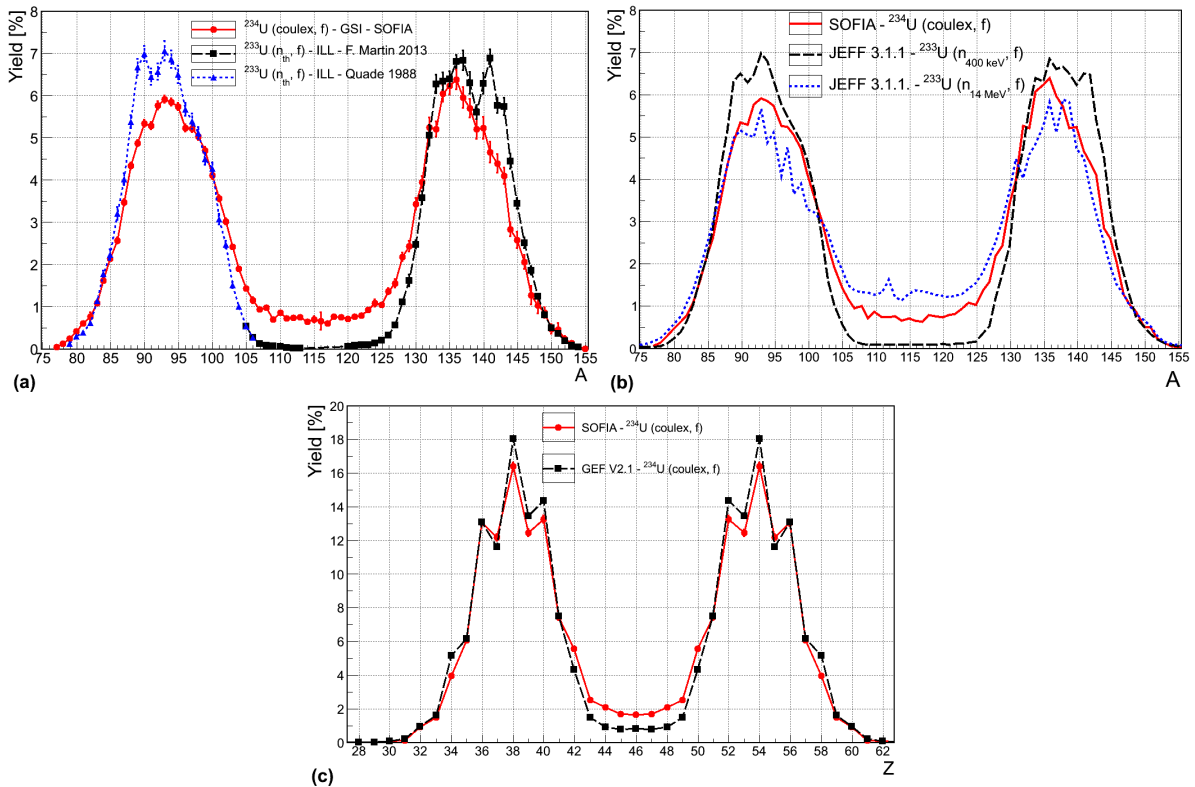


Fig. 3. (Color online) Comparison of ^{234}U fission yields with existing experimental data (a), evaluations (b) and codes (c)

The mean value has been computed for the Coulex-induced fission of ^{235}U and found to be $\bar{\nu} = 3.71 \pm 0.01$. $\bar{\nu}$ is plotted as a function of the charge of the fragments in Fig. 4 (a). It ranges from 3.5 neutrons for asymmetric fissions up to 6 neutrons for symmetric fissions ($Z = 43 - 49$). Such a behavior is explained by the different modes at play in fission. Symmetric configurations correspond to the Super Long (SL) mode of fission for which the path from saddle to scission is very long, and both nascent fragments are highly deformed. After the scission, the deformation energy is converted into excitation energy itself released through neutron evaporation. Asymmetric fission on the contrary cover both Standard one (ST1) and Standard two (ST2) fission modes, characterized by a shorter path to fission, and smaller deformation of the fragments leading to smaller excitation energy, thus lower emission of neutrons. The mean neutron multiplicity does not only represent a signature of the excitation energy of the fissioning system but is also highly dependent on the scission configuration.

4.2. Total Kinetic Energy

Computing the TKE requires to precisely determine the kinematics at the location of the fission, and in the center-of-mass of the fissioning system. The measured velocity of the beam and those of the respective fission fragments correspond to a mean kinetic energy over their respective flight path. To evaluate the "true" kinetic energy at the location of fission, corrections need to be performed to take into account the energy loss through each layer of material, before applying Lorentz transformation. The estimated mean value for the ^{235}U fissioning system is $166.2 \pm 2 \text{ MeV}$. TKE as a function of the charge of the fragments is drawn in Fig. 4 (b), and is fully consistent with what is obtained for prompt neutron multiplicity. Indeed due to the high deformation of the nascent fragments in the SL mode, the distance between their respective center-of-mass is long and consequently the Coulomb repulsion is weak, accounting for the smaller TKE values in the symmetric region. On the contrary the ST1 mode is very compact with a quasi-spherical

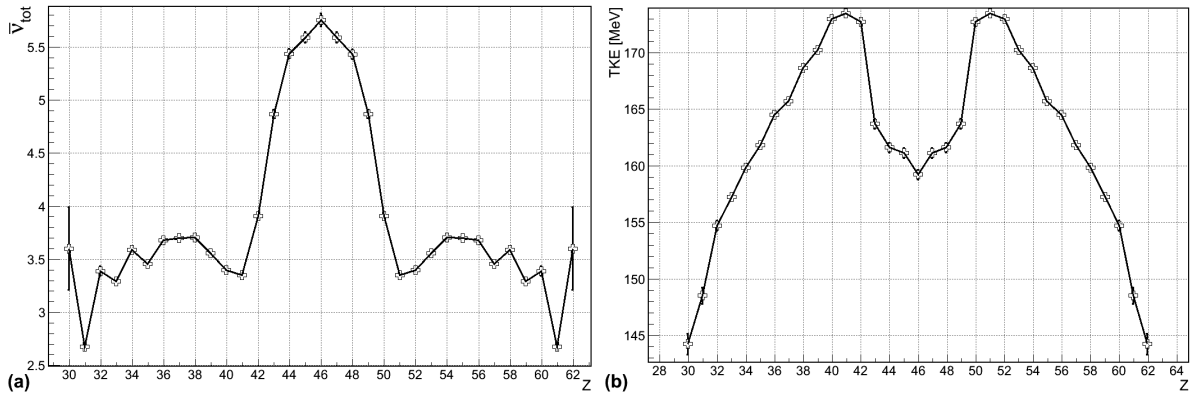


Fig. 4. $^{235}\text{U}(\text{Coul}, f)$ - (a) \bar{v} vs. Z -value of the fragments ; (b) TKE vs. Z -value of the fragments (only the statistical uncertainty is drawn)

heavy fragment (double shell closure at $Z = 50$, $N = 82$) resulting in a shorter distance and a stronger Coulomb repulsion. The importance of this effect is given by the 15 MeV gap between symmetry and asymmetry.

5. Conclusion

SOFIA (Studies On Fission with Aladin) is an innovative experimental program on nuclear data measurements at GSI. A first experiment was performed in August 2012 to study the electromagnetic-induced fission of neutron-deficient actinides and pre-actinides. The setup allows a complete identification in charge (0.4 unit FWHM) and mass (0.6 – 0.8 unit FWHM) of both fission fragments, thus enabling highly accurate measurements of fission fragments yields. Main drawback is the impossibility to have a precise value of the excitation energy on an event-by-event basis. As explicitly written in the title of this proceedings, it only refers to a small sample of our results obtained in the 2012 campaign. Indeed we have measured many other fissioning systems. Among them $^{234,235}\text{U}$ and $^{237,238}\text{Np}$ have been studied with high statistics and detailed results will be published soon. The TKE per isotope is for instance a wide source of information on its own... We have also studied the fission of neutron-deficient light actinides from ^{211}Ra down to ^{183}Hg . The statistics for these exotic fissioning systems is quite low but sufficient to infer charge distributions and have an insight at the badly-known region of the table of nuclides with a ratio N/Z below 1.4. This study is motivated by the discovery of a new type of asymmetric fission in beta-delayed fission of proton rich-nuclei [Andreyev et al. (2010)] , e.g. $^{180}\text{Tl}(\beta, f)$. In October 2014, we performed a second experiment, with an upgraded setup, in order to measure the Coulomb-induced fission of ^{236}U , which is of great interest for nuclear applications.

References

- Ebran, A. et al. NIM A 728 (2013) 40-46.
- Pellereau, E. et al. EPJ Web of Conferences 62 (2013) 06005.
- Boutoux, G. et al. Physics Procedia 47 (2013) 166-171.
- Heckman, H. H. et al. Phys. Rev. Lett. 28 (1972) 926-929.
- Quade, U. et al. Nuclear Physics A 487 (1988) 1-36.
- Martin, F. et al. Nuclear Data Sheets 119 (2014) 328-330.
- Schmidt, K.-H., Jurado, B., Amouroux, C. NEA Data Bank, JEFF Report 24 (2014)
- Andreyev, A.N. et al. PRL 105 (2010) 252502